



## Durability of an Orthesis in PLA Manufactured by the FFF 3D Printing Technology

---

Atidel Ghorbel, Adama Traore and Ahmed Elloumi

EasyChair preprints are intended for rapid dissemination of research results and are integrated with the rest of EasyChair.

November 6, 2023

## **Durability of splint arm manufactured by the FFF 3D printing technology**

Atidel GHORBEL\*, Adama TRAORE, Ahmed ELLOUMI

**\* Laboratory of Electromechanical Systems (LASEM), National Engineering School of Sfax, University of Sfax, Sfax 3038, Tunisia**

### **Abstract**

The objective of this work was to evaluate and compare the durability of 3D printing polylactic acid and the changes in mechanical and fracture behaviors due to sweat and water absorption. Beam were printed in edge direction with different angle ( $0^\circ, 45^\circ, 90^\circ$ ) and 60% of density. Beams were immersed in water and sweat for 15 days. The FFF specimens' behavior are investigated via mechanical testing (flexural test), as well as through optical analyses before and after aging.

A direct relationship between sweat and water absorption and reduction in flexural properties was observed for the PLA specimens, with the flexural modulus decreasing after 15 days of immersion. The most significant reductions were observed for specimens printed with  $45^\circ$  and in water environmental aging. The best choice of the raster angle for the splint arm manufacturing is  $0^\circ$ .

**Keywords:** 3D printing; arm splint; mechanical; sweat and water aging; durability

## 1. INTRODUCTION

The FFF (Filament Fused Fabrication), is among the well-known 3D printing technology that was used in different field especially the biomedical application, enabling the creation of complex geometries with specific properties [1-2]. Many service factors could influence the mechanical properties of 3D printed parts depending on the structural performance.

Splint arm in Polylactic acid (PLA), where recently manufactured by FFF technology [3-4]. Polylactic Acid (PLA), derived from renewable resources, is a widely used biocompatible material in biomedical applications. Its mechanical properties and affordability make it a popular choice compared to other materials. PLA also offers advantages like hydro massage compatibility, invisibility in x-rays, and recyclability for filament production [5].

One limitation of 3D printed polymeric orthosis like PLA splint arm is degradation with sweat and humidity as they can diffuse through the pores and layers of the final component. PLA, being hydrophobic, can degrade under hydrolytic conditions caused by the diffusion of water molecules and subsequent ester bond breakage. Several studies have investigated the effects of printing parameters, such as layer thickness and orientation, on water absorption rates and mechanical properties of PLA [6]. The printed PLA leads to higher water absorption of PLA than other industrial processes. The main absorption of the Printed PLA in different water solutions happened during the first three or four days [7]. Additionally, the properties degradation after water absorption are influenced by the building orientation and raster angle [6].

Until now, there is currently no research compared the effect of sweat and water on the degradation and also on the mechanical properties of 3D printed parts. In this study, we focused on studying a bending specimens printed in the on-edge direction, varying the raster angle with 60% infill density. We examined the mechanical properties in relation to the raster angle and the environmental conditions (distilled water or sweat). The findings provide valuable insights into the effects of sweat and humidity interaction on mechanical performance and fracture behavior of PLA printing arm splints

## 2. MATERIALS AND METHODS

### 2.1. Fabrication of arm splint

In the first time, arm splint for this study were fabricated via FFF 3D printing (see figure 1). We decided to position the splint vertically on the build plate, which required the use of supports. We utilized a layer thickness of 0.4 mm.

### 2.2. Materials

Specimens for this study were fabricated (FFF) 3D printing with dimensions  $85 \times 10 \times 4$  mm<sup>3</sup>. Polylactic acid (PLA) specimens were printed using Ender 5 Pro 3D

printer and Nipovas PLA filament (Diameter: 1.75 mm). All the specimens were printed in an “on edge” construction orientation with an infill density of 60%. Other process parameters were fixed level such as layer thickness (0.4 mm), fill pattern (rectilinear) and temperature (220°C). All controlled printing parameters are collected in Table 1.

### 2.3. Sweat and water absorption study

Sweat and water absorption analysis were performed on the bending PLA samples. Each specimen was fully immersed in artificial sweat [2] or distilled water at 21 °C. The pH of the sweat solution is 5,5. Before degradation, the initial weight ( $M_i$ ) of 3D-printed PLA specimens were measured using an analytical balance (AS-R2-plus (RADWAG)) with precision of  $\pm 0.0001$  g. Periodically, with times ranging from 1 to 15 days, the specimens were removed, carefully dried with a paper towel, and their mass recorded

The mass percent change is then calculated using Equation 1:

$$M\% = \frac{Mt - Mi}{Mi} \times 100 \quad (1)$$

Where:

- M : the percentage of sweat or water absorption.
- Mt : mass of specimen (grams) after time t.
- Mi : initial mass (grams) of specimen.

### 2.4. Flexural testing

The PLA specimens for three point bend flexural tests were prepared according to NF T51-120 at room temperature. The maximum load capacity of the equipment is 5 KN. The following processing conditions were considered.

- Varing the raster orientation angle through edge (0°, 45° and 90°).
- Environmental conditions (distilled water (pH 7) or sweat (pH 5.5)).

A schematic of the flexure specimen is shown in figure 2. After immersion, the specimens were weighed and tested at a displacement rate of 5 mm/min with a support span of 65 mm. Virgin specimens were also tested. Five tests were carried for each processing condition and an average value is reported.

### 2.5. Microstructural study

To better understand the effects of aging environment on failure modes of specimens, microscopic inspection was performed utilizing a BRESSER digital microscope with a magnification cell (20x80x350). All microstructural features are carried out after flexural tests.

### 3. MAIN RESULTS

Following the conducted tests, results of the analyses of the selected properties of samples prior to degradation were obtained. In addition, results of the impact of aging pH solution on the selected mechanical and structural properties of PLA were recorded.

The mechanical response of the non-aged specimens was evaluated by means of bending tests (see Figure 4). These tests showed that the variation in the raster orientation angle has a significant effect on the mechanical properties. The specimens printed at an angle of 45° show better mechanical resistance ( $F_{max}: 89 \pm 19,03 \text{ N}$ ) and a higher modulus ( $2137,9 \pm 105,26 \text{ MPa}$ ). For this case, the filaments behave as solid barriers that prevent and slow the propagation of cracks and therefore lead to higher resistance. Microscopic analysis confirmed these results. Indeed, the observation of the fracture surfaces show that in the case of specimens printed at an angle of 45°, the geometry of the contour as well as the diameter of the filaments and the distance between the filaments do not change. Failures occurred along the direction of the raster when it was at a 45° angle. Figure 7 showed that fractures initiated at different layers between the rasters due to shear forces and then propagated through the layer interface.

In the 0° raster angle, greater displacements were observed (9.1 mm). Other research found that 00° raster angle samples lead to increased ductility in tensile tests [9] as filaments support the loads in the longitudinal direction. Microscopic analysis showed that fractures occurred in the transverse direction of the filaments within each layer. There are pores and voids between the strands of each layer, leading to trans-raster failure [10].

The mechanical properties are expected to be the weakest at 90° raster angle as the forces tend to separate the strands in each layer and between layers. The maximum forces and modulus of PLA-90° are respectively  $45,4 \pm 3,4 \text{ N}$  and  $1709,42 \pm 42,89 \text{ MPa}$ . The microscopic analyses displays an inter-raster fusion failure (figure 8).

To summarize, there were two main failure modes for the tested samples: (1) Inter-raster fusion failure, in the case of PLA-45° and PLA-90° (2) Trans-raster failure, in the case of PLA-00° [11]. The samples with 45° raster angle sustained the highest flexural properties. The main question here was whether the behavior of these samples remains the same after aging.

Printed specimens were subjected to water and sweat absorption to assess the mechanical properties in real application. The study of the effect of ageing by artificial sweat and distilled water showed that after 15 days the specimens did not show the same rate of absorption. Figure 3 shows that for a fixed raster angle there is an increase of absorption in the case of distilled water solution. This result is validated by the microscopic observations (figure 7). In fact, hydrolytic water effect enhances the interface between printed layers more than the case of sweat.

Higher absorption is observed in the PLA-90°. Elsewhere, 45° raster angle exhibited lower water or sweat absorption. This could be explained by the fact that the

type and distribution of the porosity change with raster angle or by the orientation of inter-layer that protected the printed part.

The mechanical response of aged specimens in the case of 45°angle prove significantly degradation in the mechanical strength even if it presents the lowest absorption. We noted a decrease in strength and rigidity (figure 4 and 5). The flexural properties are more affected in the case of distilled water aging solution ( $E = 1548,32 \pm 308,39$  MPa in sweat solution and  $E = 1037,2 \pm 304,74$  MPa in water solution). The observation of the first surface of contact with the distilled water in this case shows that water aging has a significant effect on the acceleration of the damage phenomena. Figure 7 reflects large porosities between construction plans. This leads that the inter-layers adhesion became weak by ageing the PLA specimens for 15 days.

However, the specimens printed at an angle of 90° had a greater absorption rate of sweat and distilled water (figure 3), showed lower decrease in stiffness and strength (figure 4 and 5). A similar mechanical results are observed in the PLA-00° samples. These results are in agreement with those of microscopic observation. Figures 6 and 8 shows the similar fracture morphology of surface fracture. Just a plasticization zone due to water absorption are observed.

This study permits the best choice of the parameters for the splint arm manufacturing. For a infill density of 60%, the best raster angle is 0°.

#### **4. CONCLUSION**

This study compares the effects of sweat and water absorption on the durability of commonly used 3D printing polylactic acid in orthotics applications. 3D printed specimens were prepared and changes in their morphological and mechanical behavior were evaluated. The investigation into these properties revealed the impact of the raster angle and the nature of aging solution. The most significant reductions were observed for specimens printed with 45° and in water environmental aging. Plasticization and eventual more porosities due to water absorption resulted in significant losses in mechanical properties.

#### **5. MAIN REFERENCES**

- [1] M. Walbran, K. Turner, et A. J. McDaid, « Customized 3D printed ankle-foot orthosis with adaptable carbon fibre composite spring joint », *Cogent Eng.*, vol. 3, n° 1, p. 1227022, déc. 2016, doi: 10.1080/23311916.2016.1227022.
- [2] M. Vignesh *et al.*, « Development of Biomedical Implants through Additive Manufacturing: A Review », *J. Mater. Eng. Perform.*, vol. 30, n° 7, p. 4735-4744, juill. 2021, doi: 10.1007/s11665-021-05578-7.

- [3] P. Guida et al., « An alternative to plaster cast treatment in a pediatric trauma center using the CAD/CAM technology to manufacture customized three-dimensional-printed orthoses in a totally hospital context: a feasibility study », *J. Pediatr. Orthop. B*, vol. 28, no 3, p. 248-255, mai 2019, doi: 10.1097/BPB.0000000000000589.
- [4] A. Dal Maso et F. Cosmi, « 3D-printed ankle-foot orthosis: a design method », *Mater. Today Proc.*, vol. 12, p. 252-261, janv. 2019, doi: 10.1016/j.matpr.2019.03.122.
- [5] T. Casalini, F. Rossi, A. Castrovinci, et G. Perale, « A Perspective on Polylactic Acid-Based Polymers Use for Nanoparticles Synthesis and Applications », *Front. Bioeng. Biotechnol.*, vol. 7, 2019, Consulté le: 7 juin 2023. [En ligne]. Disponible sur: <https://www.frontiersin.org/articles/10.3389/fbioe.2019.00259>
- [6] N. Ayrilmis, M. Kariz, J. H. Kwon, et M. Kitek Kuzman, « Effect of printing layer thickness on water absorption and mechanical properties of 3D-printed wood/PLA composite materials », *Int. J. Adv. Manuf. Technol.*, vol. 102, n° 5, p. 2195-2200, juin 2019, doi: 10.1007/s00170-019-03299-9.
- [7] D. Moreno Nieto, M. Alonso-García, M.-A. Pardo-Vicente, et L. Rodríguez-Parada, « Product Design by Additive Manufacturing for Water Environments: Study of Degradation and Absorption Behavior of PLA and PETG », *Polymers*, vol. 13, n° 7, p. 1036, janv. 2021, doi: 10.3390/polym13071036.
- [8] C. Dubois, J. Verbrel, V. Rigny-Bourgeois, Y. Grohens, « Photo-Ageing of a thermoplastic polyurethane in contact with artificial Sweat », *Macromol. Symp.*, 2003, 203, pp.325-330.
- [9] M. Algarni et S. Ghazali, « Comparative Study of the Sensitivity of PLA, ABS, PEEK, and PETG's Mechanical Properties to FDM Printing Process Parameters », *Crystals*, vol. 11, n° 8, p. 995, août 2021, doi: 10.3390/cryst11080995.
- [10] B. Rankouhi, S. Javadpour, F. Delfanian, et T. Letcher, « Failure Analysis and Mechanical Characterization of 3D Printed ABS With Respect to Layer Thickness and Orientation », *J. Fail. Anal. Prev.*, vol. 16, n° 3, p. 467-481, juin 2016, doi: 10.1007/s11668-016-0113-2.
- [11] Souissi S, Bennour W, Khammassi R, Elloumi A. Mechanical properties of 3D printed parts: Effect of ultraviolet PLA filaments ageing and water absorption. *Journal of Elastomers & Plastics*. 2022;0(0). doi:10.1177/00952443221144736.

**Table 1.** Controlled printing parameters

Parameter	
Infill density (%)	60
Feed rate (mm/s)	60
Extruder temperature (°C)	220
Bed temperature (°C)	60
Number of shells	1
Build orientation	On-edge
Fill pattern	Rectilinear
Raster angle (°)	0, 45 and 90
Layer height (mm)	0,3
Top/bottom	none

**Figure 1.** 3D printing of arm splint.

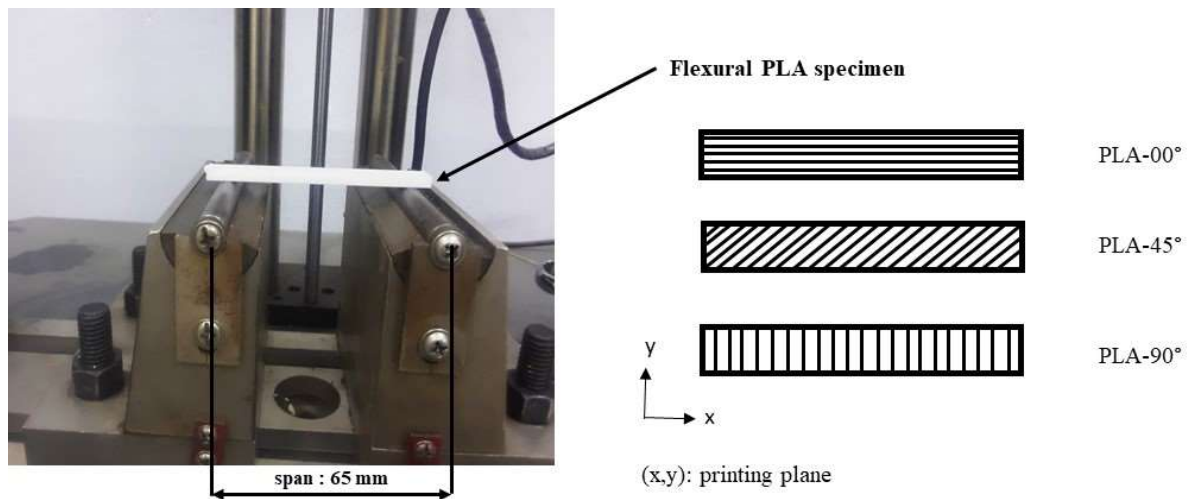


**Figure 2.** Flexural test of 3D printed specimens with different raster angle.

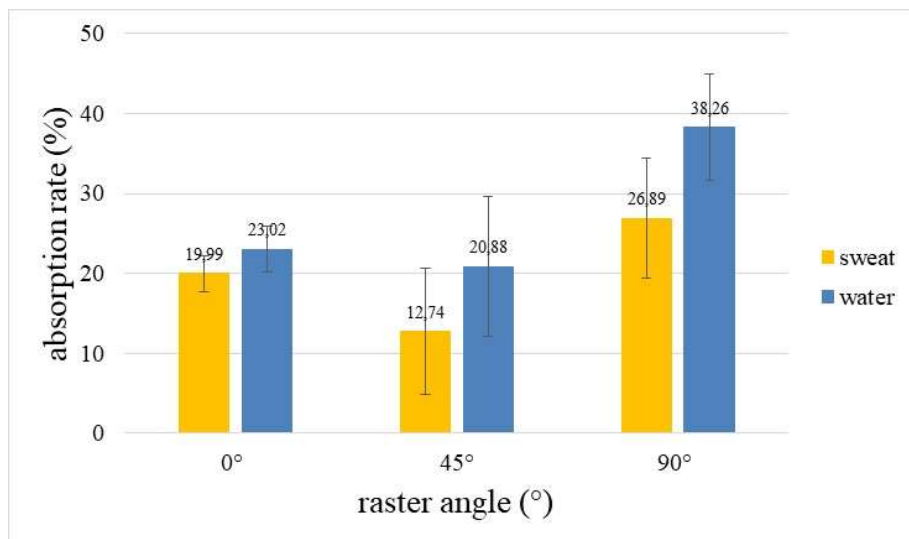


**Figure 3.** Sweat and water absorption results for immersed specimens

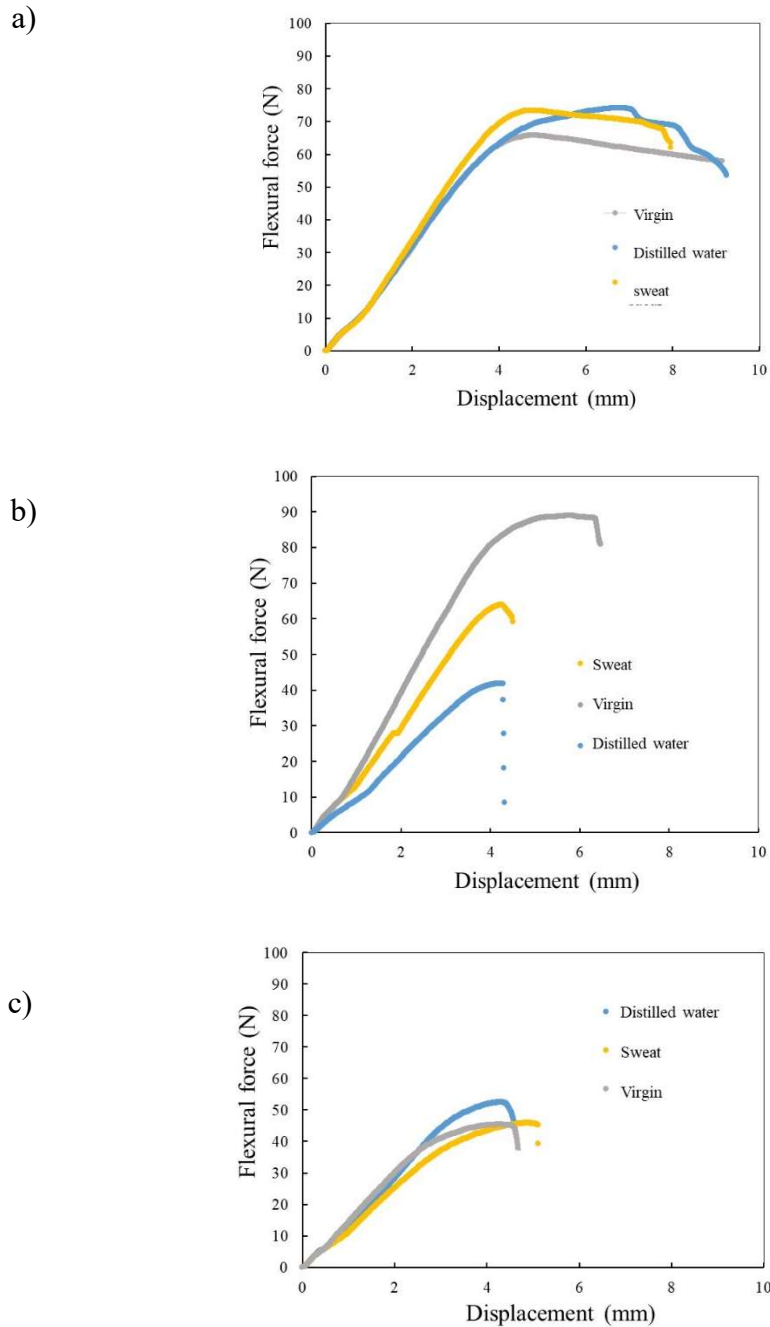


**Figure 4.** Representative flexural force versus flexural displacement plots for: (a) PLA-00°, (b) : PLA-45° and (c) : PLA-90°.

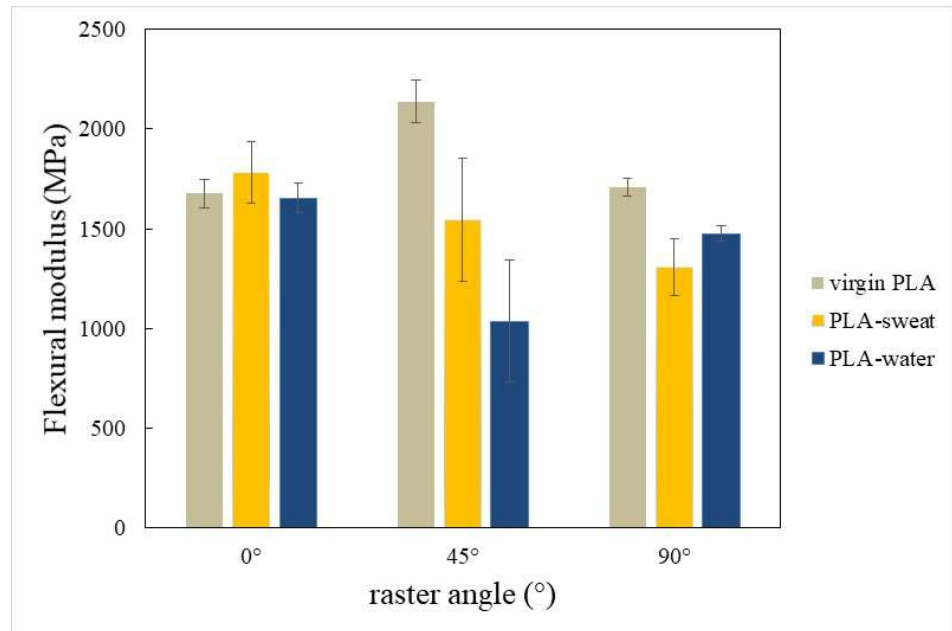


**Figure 5.** Flexural modulus before and after exposure to artificial sweat and distilled water.

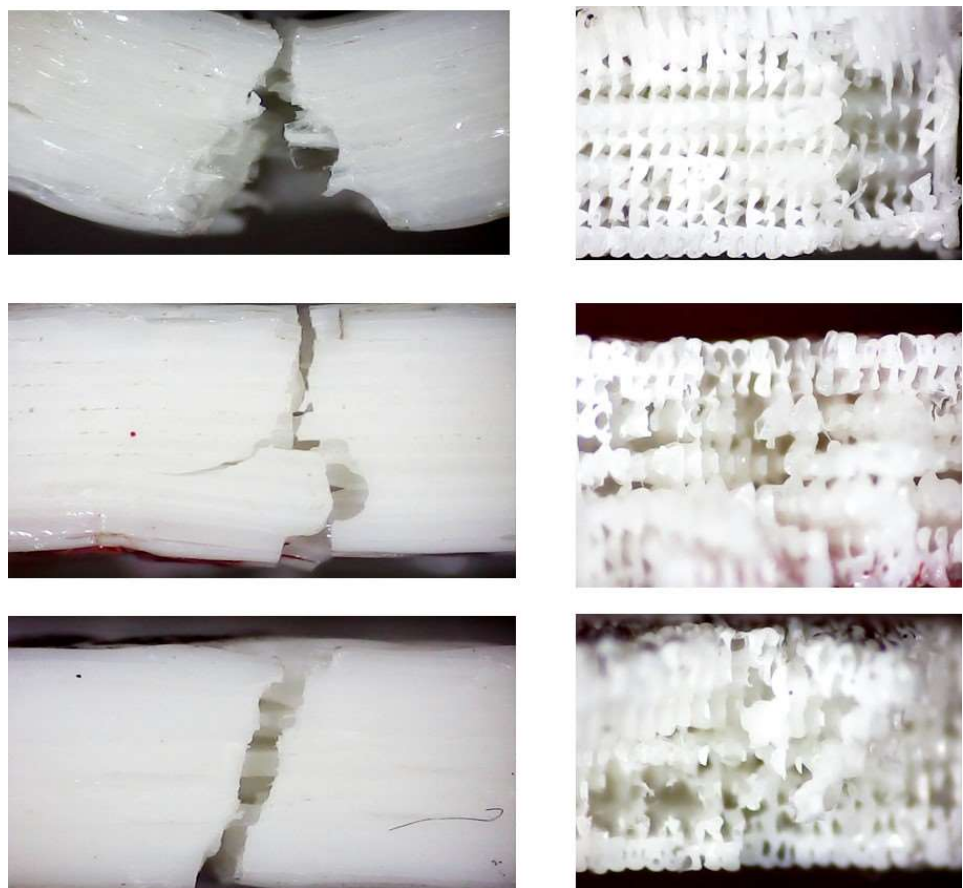


**Figure 6.** Microscopic inspection of air gaps between rasters and layers in the case of PLA-00° specimens (a) before aging, (b) in distilled water and (c) in artificial sweat.

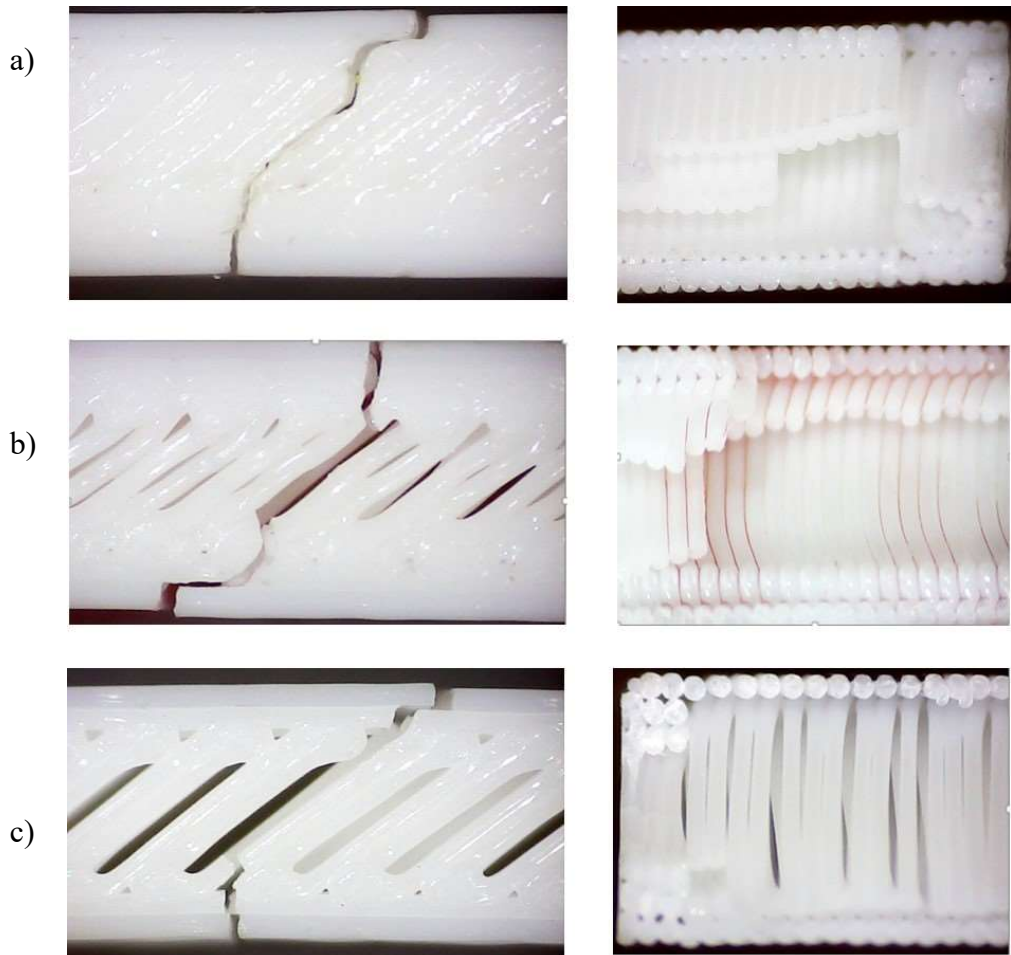


**Figure 7.** Microscopic inspection of air gaps between rasters and layers in the case of PLA-45° specimens (a) before aging, (b) in distilled water and (c) in artificial sweat.

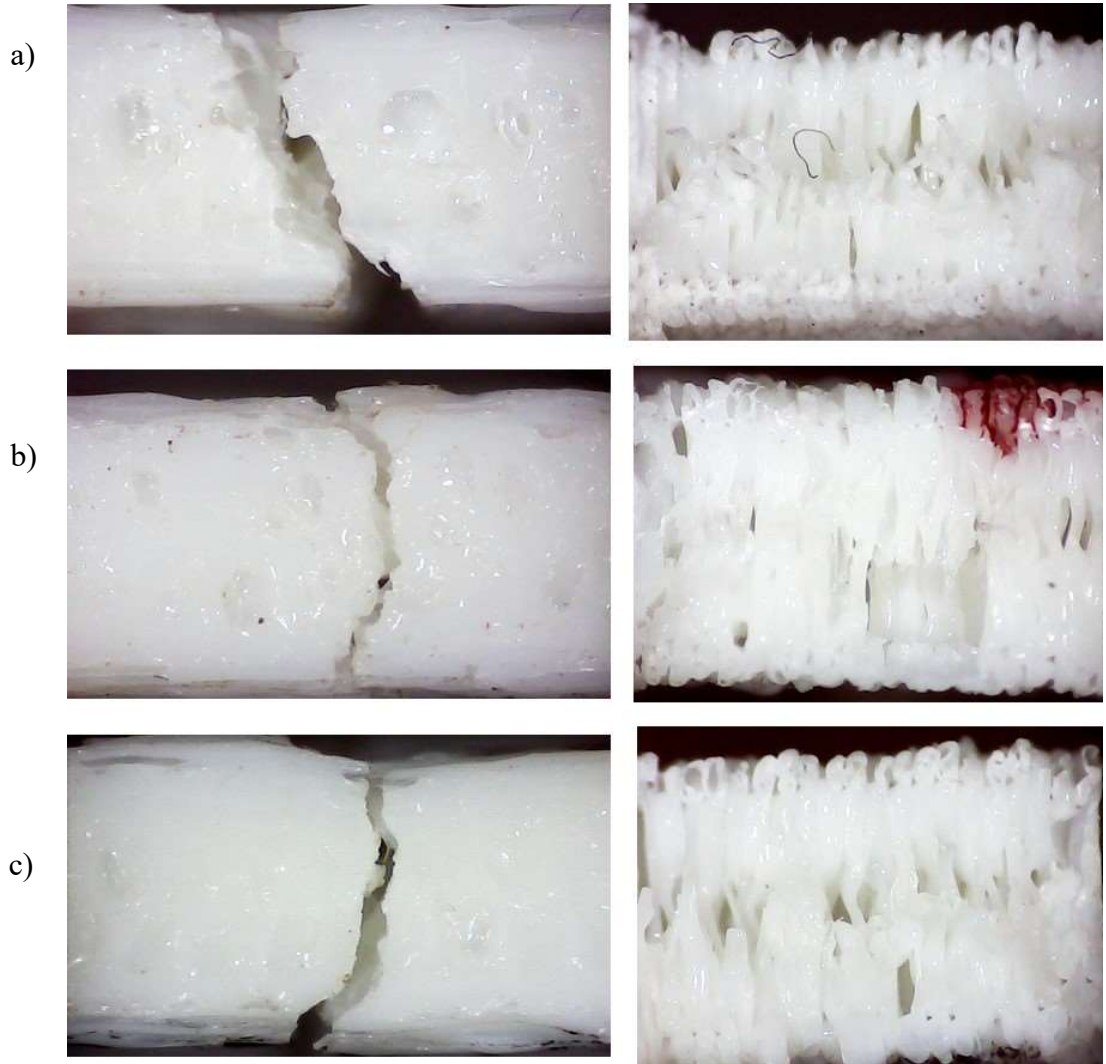


**Figure 8.** Microscopic inspection of air gaps between rasters and layers in the case of PLA-90° specimens (a) before aging, (b) in distilled water and (c) in artificial sweat.